Low Temperature Physics

Piezoelectric response in SmFe$_3$(BO$_3$)$_4$, a non-piezoactive configuration. The surface piezoelectric effect

M. P. Kolodyazhnaya, G. A. Zvyagina, I. A. Gudim, I. V. Bilych, N. G. Burma, K. R. Zhekov, and V. D. Fil

View Online   Export Citation   CrossMark

ARTICLES YOU MAY BE INTERESTED IN

Magnetocapacitance, magnetoelasticity, and magnetopiezoelectric effect in HoFe$_3$(BO$_3$)$_4$
Low Temperature Physics **44**, 1341 (2018); https://doi.org/10.1063/1.5078631

Single crystals growth of hexaferrits M-type MTi$_x$Co$_x$Fe$_{12-2x}$O$_{19}$ (M=Ba, Sr) by floating zone and investigation of their magnetic and magnetoelectric properties
Low Temperature Physics **43**, 971 (2017); https://doi.org/10.1063/1.5001298

Surface piezoelectricity: Size effects in nanostructures and the emergence of piezoelectricity in non-piezoelectric materials
Journal of Applied Physics **110**, 104305 (2011); https://doi.org/10.1063/1.3660431

Piezoelectric response in SmFe₃(BO₃)₄, a non-piezoactive configuration. The surface piezoelectric effect

M. P. Kolodyazhnaya and G. A. Zvyagina

B. Verkin Institute for Low Temperature Physics and Engineering, NAS Ukraine, 47 Nauka Ave., Kharkov 61103, Ukraine

I. A. Gudim

Kirensky Institute of Physics, Siberian Branch, Russian Academy of Sciences, 50 Akademgorodok St., Krasnoyarsk 660036, Russia

I. V. Bilych, N. G. Burma, and K. R. Zhekov

B. Verkin Institute for Low Temperature Physics and Engineering, NAS Ukraine, 47 Nauka Ave., Kharkov 61103, Ukraine

V. D. Fil[a)]

Kirensky Institute of Physics, Siberian Branch, Russian Academy of Sciences, 50 Akademgorodok St., Krasnoyarsk 660036, Russia
(Submitted February 3, 2017)

An investigation of the mechanisms responsible for the manifestation of the piezoelectric effect in configurations that should not allow for piezoelectric response in the paramagnetic state due to their symmetry. In spite of these symmetry constraints the existence of such a piezoelectric response is detected in this study. It is assumed that these results are associated with the surface on which symmetry constraints are absent. In the magnetically ordered state an indirect piezoelectric effect is both symmetrically permissible and actually observable in these configurations, and it consists of the combined effects of magnetoelectric and magnetoelastic mechanisms. *Published by AIP Publishing.* [http://dx.doi.org/10.1063/1.5001291]

The classical piezoelectric effect (PE) linearly couples the electric field **E** and elastic deformation u_{kl}.[1] In the thermodynamic potential, the PE is represented by terms such as $e_{i,kl}E_i u_{kl}$. The piezomodulus tensor $e_{i,kl}$ is symmetric with respect to the last two indices and is usually written in Voigt notation. The structure of the tensor e_{ij} ($j = 1, …, 6$) is determined by the symmetry of the crystal lattice. The bulk PE is possible only in the absence of an inversion center. Other symmetry operations determine the number of non-zero components of the e_{ij} tensor. In crystal class 32, which is discussed below and to which most ferroborates belong, only five components are non-zero.[1]

The set of orientations of external (and internal) fields, for which $e_{ij} \neq 0$, will be referred to as the piezoactive configuration. These include the deformation u_{xx} that generates the E_x field (configuration E_x, u_{xx}), or u_{xy}, which generates the E_y field (configuration E_y, u_{xy}).[1] At the same time the component $e_{22} \equiv e_{y,yy} = 0$, since during a 180° rotation around the $C_2 || x$ axis it changes signs, and the deformation u_{yy} does not lead to the appearance of the E_y field, i.e., the configuration E_y, u_{yy} is not piezoactive.

In addition to the aforementioned direct PE, in magnetically ordered media that belong to the class of multiferroics, the existence of an indirect PE is also possible, which consists of the joint action of the magnetoelastic and magnetoelectric mechanisms. Because of magnetoelasticity, the deformation changes the state of the magnetic variables and excites the electric field (and vice versa) through magnetoelectric coupling. This effect was first discovered in samarium ferroborate.[2] Due to the easy-plane configuration of the antiferromagnetic phase, the field variables relatively easily modulate the angular position of the magnetic vectors, which is what causes the gigantic magnitude of the effect— the effective piezomodulus in SmFe₃(BO₃)₄ increases more than twofold. The constant magnetic field changes both the position of the magnetic vectors and the depth of its modulation. As a result fields that are several Tesla in magnitude suppress this type of PE, and therefore it has been named "magnetopiezoelectric."

Note also the possibility of direct renormalization of the direct PE involving magnetic vectors. In the class of easy-plane ferroborates interaction of this sort is accounted for in the thermodynamic potential by terms such as $\tilde{e}_{imn,kl}E_i u_{kl}l_m l_n$, where l_m, l_n are the direction cosines that define the positon of the antiferromagnetism vector in the easy plane. Evidence of such a process is detected in neodymium ferroborate,[3] however the renormalization of the piezomodulus does not exceed 1%.

The references cited above are related to the study of the magnetopiezoelectric effect in piezoactive configurations. In reality, this circumstance as it applies to multiferroics, is not mandatory. Under magnetic ordering the total symmetry decreases relative to the crystallographic order, as a result of which the manifestation of the piezoelectric response becomes possible in non-piezoactive configurations. This study puts forth the phenomenological arguments and

experimental results of studying such a situation for the specific geometry of $SmFe_3(BO_3)_4$. The change to the elastic modulus in this case is also considered. The most interesting and least expected result is the discovery of a new channel of piezoelectric response formation, which is assumed to originate from the surface and thought to exist in both a magnetically ordered state and in the paraphase.

The behavior of the piezomodulus in the non-piezoactive configuration E_y, u_{yy} is analyzed. The material can be conveniently discussed in comparison to the PE characteristics in the piezoactive configuration E_x, u_{xx}. The main results for the latter case are laid out in detail in Ref. 2, and they will be used in this study as necessary.

The actual part of the incomplete thermodynamic potential that makes it possible to make the necessary estimates, can be written as[2]

$$\tilde{F} = K\cos 6\varphi + e_{11}E_x u_{xx} + \frac{a}{2}(E_x \cos 2\varphi - E_y \sin 2\varphi)$$
$$+ \frac{b}{2}(u_{xx} - u_{yy})\cos 2\varphi - \frac{1}{2}\chi H^2 \sin^2(\varphi_H - \varphi). \quad (1)$$

Here φ is the angle between the antiferromagnetism vector and the x axis, φ_H is the angle between the external field H and the x axis, e_{11} is the piezomodulus, and χ is the magnetic susceptibility. The first term in Eq. (1) is the anisotropy in the reference plane and the second is the direct PE (note the absence of the term with e_{22}), the third and fourth are the magnetoelectric and magnetoelastic contributions, respectively, and the last term is the Zeeman energy. The interaction responsible for the flexoelectric effect will be discussed below.

The piezomodulus is calculated according to the following:[1] $\sigma_{kl} = \partial \tilde{F}/\partial u_{kl}$; $e_{ikl} = d\sigma_{kl}/dE_i$ (wherein σ_{kl} is a component of the stress tensor). When performing the second differentiation it is necessary to account for the fact that φ is an implicit function of E (as well as of u). As a result, we obtain the following for the effective piezomoduli:

$$\Delta e_{11} = e_{11}^{eff} - e_{11} = -\frac{ab\sin^2 2\varphi}{\partial^2 \tilde{F}/\partial\varphi^2}, \quad (2)$$

$$e_{22}^{eff} = -\frac{ab\sin 4\varphi}{2\partial^2 \tilde{F}/\partial\varphi^2}. \quad (3)$$

Here and hereinafter e_{11} will be understood as the value of the tensor component in the paraphase.

In the absence of an external magnetic field a uniform sample below the Néel (T_N) temperature will break into domains that retain the initial symmetry of the paraphase on a macroscopic level. Averaging Eqs. (2) and (3) over the whole sample, we can see that the division of the configuration into piezoactive and non-piezoactive below T_N is conserved and e_{22}^{eff} (as opposed to Δe_{11}), as expected, is reset. However, in each individual domain, e_{22}^{eff}, with the exception of select φ values, has a non-zero value. This in no way contradicts the symmetry argument because in each antiferromagnetic domain the initial symmetry of the paraphase is already lost.

Let us now present the experimental results and their discussion. The method of measuring the piezomodulus is described in detail in Ref. 2. We will note only the details that are important to this discussion. All measurements were performed in pulsed mode. The elastic wave is introduced to the test sample through a delay line consisting of a Mo single crystal with the direction of the wave normal along the [110] axis. The delay material is sufficiently contaminated so as to suppress the electron contribution to the sound propagation characteristics at the utilized frequencies ($\sim$55 MHz). The potential arising at the input interface of the sample as a result of the piezoelectric interaction goes to the low-resistance ($\sim$50 Ohm) receiver input during the time of the electromagnetic delay in the sample (retarded potential). As argued in Ref. 2, the amplitude of the received signal in such a case is proportional to the piezoelectric modulus. The thickness of the test samples was chosen to be $\sim$3 mm, which provided a sound delay of at least 0.3 μs and made it possible to separate the analyzed signal from the piezoelectric response generated by the elastic wave arriving at the output interface.

At $H = 0$ in the magnetically ordered phase, partial concentrations of different domains on the excitation interface (plane (010)) depend on the prior history, boundary defects, cooling rate, and other factors that are difficult to control. For these reasons the response in configuration E_y, u_{yy}, as opposed to e_{11}^{eff} (see Ref. 2) displayed irregular bursts during temperature scanning, which are not reproducible in different cooling cycles. It was not possible to catch any sort of regularity in its behavior and we will not be presenting this data.

All of the results discussed below refer primarily to the single-domain spin-flop state realized in fields $H > 1$–1.5 T. Recall that in this state $\varphi \approx \varphi_H + \pi/2$. Figure 1 shows the behavior of the amplitude and phase of the piezoelectric response in the configuration E_y, u_{yy} as a function of φ_H at $T = 1.7$ K. For a more detailed reproduction in the small amplitude region the results are given in logarithmic coordinates. There is almost complete agreement between the behavior of the response E_y and Eq. (3); the amplitude is periodic with the period close to $\pi/4$, and the phase with the same periodicity changes by $\pm 180°$. The signal maxima are observed at $\varphi_H \approx (2n + 1)(\pi/8)$ ($n = 0,1,2...$) The relatively large value ($-(15$–17) dB) of the minimum amplitude of the response, turned out to be a surprise. According to the
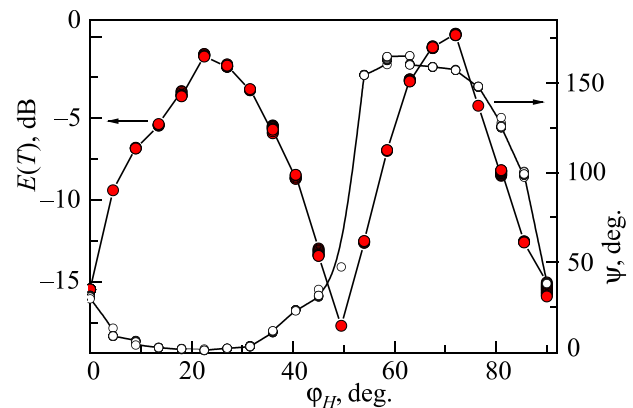

Fig. 1. The dependence of the amplitude and phase of the piezoelectric response on the orientation of the magnetic field ($H = 1.2$ T) in the reference plane. The filled in symbols represent the amplitude, the open symbols are the phase. Lines are drawn as visual aides.
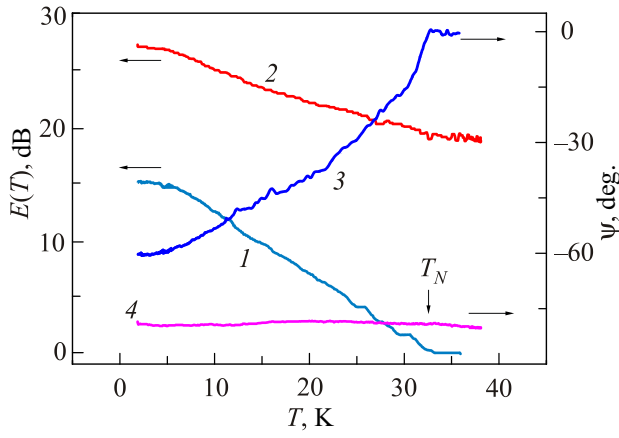
Fig. 2. The temperature variations of amplitudes (*1, 2*) (logarithmic scale) and phases (*3, 4*) of the responses in non-piezoactive (*1, 3*) and piezoactive (*2, 4*) configurations, given optimal values of φ_H that provide the maximum response amplitude ($\varphi_H = \pi/8$ for the configuration E_y, u_{yy}, and $\pi/4$ for the configuration E_x, u_{xx}). $H = 1.4$ T. All values are calculated based on the values at $T = T_N$ in the configuration E_y, u_{yy}.

considerations noted above a much deeper minimum was to be expected.

Figure 2 shows the initial experimental results that represent the temperature variations of the response amplitudes (on a logarithmic scale) and phases in piezoactive and non-piezoactive configurations. These results were obtained for optimal values of φ_H which provide the maximum response amplitude ($\varphi_H = \pi/8$ for the configuration E_y, u_{yy}, and $\pi/4$ for the configuration E_x, u_{xx}). The relative changes to the discussed parameters in each particular configuration are the values that are being measured directly in the experiment. Their mutual position is fairly simply determined using Eqs. (2) and (3) (see below). In particular, in Fig. 2 the amplitude and phases of the signals are calculated based on values that characterize the response in E_y at $T = T_N$. Note the following features.

1. The range of temperature variations of the amplitude E_y is close to the rotation diagram variations (compare Fig. 2, curve 1 and Fig. 1). This means that at the minimum of the rotation diagram the amplitude of the response is of an unknown nature (we will denote it as $\tilde{E}_y$) and is practically independent of temperature. Moreover, this signal exists without noticeable level changes until the melting point of the acoustic binder ($T > 100$ K, not shown on the figure), and there is no reason to believe that at any temperature it will disappear. 2. In the piezoactive configuration the phase of the signal during the transition through T_N remains practically unchanged. Therefore, our working frequency is sufficiently low in comparison to the relaxation frequencies that are typical for antiferromagnets, and the phases of both direct and indirect PE coincide. This same phase, by virtue of Eqs. (2) and (3), also characterizes the spin-dependent response in the non-piezoactive configuration. The phase of the signal $\tilde{E}_y$ at $T > T_N$ is also unchanged, and it can be assumed that even at $T < T_N$ it is conserved. However, below T_N the response of E_y undergoes significant changes to the phase ψ, in favor of a decrease ($\sim 60°$). A natural interpretation of the noted features is that in the antiferromagnetic state, the response E_y represents the sum of two signals shifted in phase with respect to each other by a fixed value

exceeding at least $\pi/3$. The phase of the resulting oscillation evolves solely as a result of the change to the ratio between the amplitudes of these signals

$$E_y = \tilde{E}_y + E_{ME} = e_{22}^{\text{res}} u_{yy} = \left[e_{y2} + e_{22}^{\text{eff}} \exp(-i\psi_0)\right] u_{yy}. \quad (4)$$

In Eq. (4) E_{ME} is understood as the field that appears as a result of the magnetopiezoelectric effect. In addition, the resulting piezomodulus e_{22}^{res} and piezomodulus e_{y2}, which couples $\tilde{E}_y$ with u_{yy} (we used a nonstandard notation, emphasizing the irregularity of this coefficient), are introduced. The temperature independent phase of the signal $\tilde{E}_y$ is taken as the origin, and the delay in E_{ME} relative to $\tilde{E}_y$ is taken into account by assigning the phase factor with a fixed value ψ_0 from Eq. (3), to the value of e_{22}^{eff}.

Let us first discuss the possible causes behind the appearance of a piezoelectric response in the non-piezoactive configuration of the paramagnetic phase that are provided for by the features of the experiment. A rather unlikely scenario is associated with the limited cross section of the sound beam. If there is a shift in the beam u_y there are definitive regions with nonzero piezoactive deformation u_{yx} at its boundaries, which are the source of the field E_y. In this case the diametrically opposite plots of the cylindrical sound beam cross section generate signals that are mutually compensated in the symmetrically located recording electrode. However when the cross section deviates from strict cylindricality (inhomogeneity of acoustic binding) there is a decompensation and this piezoelectric response mechanism, in principle, could be possible. The homogeneity of the binding is a parameter that is difficult to control, and one would expect that the results would not be reproducible across different measurement cycles, which was not actually observed. And most importantly, in this scenario it is impossible to explain the appearance of a phase shift between $\tilde{E}_y$ and E_{ME}.

The appearance of $\tilde{E}_y$ could also be caused by the deviation of the wave normal from the required direction by an inaccurate crystallographic orientation of both the sample and the delay line. However, in this case, there should be no phase shift between $\tilde{E}_y$ and E_{ME}.

The fundamental mechanisms behind the manifestation of $\tilde{E}_y$ are flexoelectricity[4] and surface piezoelectric effect.[5]

Flexoelectricity is the occurrence of polarization in a dielectric medium under the influence of inhomogeneous deformation. At low perturbations the flexoelectric coupling is expressed by a linear relationship between the polarization and the deformation gradient: $P_m = \mu_{mlik} \partial u_{ik} / \partial x_l$. The fourth rank of the flexoelectric tensor μ_{mlik} permits the existence of the effect at any symmetry, including in a centrosymmetric medium. It is easy to verify that in class 32 the component μ_{yyyy}, similar to the corresponding component of the elastic modulus tensor, is nonzero. Also note that at $\mu < 0$ the flexoelectric response is 90° ahead of the piezoelectric response. Qualitatively speaking, the relationship between the appearance of response $\tilde{E}_y$ and the flexoelectric effect is completely permissible, and the problem is reduced to a quantitative comparison. The theoretical estimates and available measurement results for a single crystal with standard values of dielectric permittivity (~ 10) show that the values of flexoelectric coefficient μ do not exceed 10^{-8} C/m (see Ref. 4, Table 2). With respect to sound, the flexoelectric interaction

formally reduces to the effective piezoelectric interaction with a frequency-dependent piezomodulus ($e^{fe} = \mu q$, q is the wave number). At the frequencies used in this article the quantity e^{fe}, in accordance with Ref. 4, does not exceed 10^{-3} C/m². Considering that in $SmFe_3(BO_3)_4$ $e_{11} \approx 1.4$ C/m²,[6] it can be seen in Fig. 2 that this value e^{fe} is more than two orders of magnitude less than the actual observed value of ($e_{y2}(T_N) \approx 0.15$ C/m²). If we do not assume that $SmFe_3(BO_3)_4$ has anomalously large flexoelectric coupling, this hypothesis should be discarded.

The term "surface piezoelectric effect" implies that it differs from the classical PE, which has a three dimensional nature. This is due to the fact that almost all symmetry elements, including the inversion center, are lost at the interface surface of the crystalline body. For example, pursuant to the geometry of the class 32 crystal being discussed, the symmetry axes of both the third and second order are "lost." The absence of symmetry constraints allows for the appearance of a piezoresponse in virtually any configuration, including in the one up for discussion, and the question is still reduced to quantitative estimates. The calculations carried out in Ref. 5 for cubic perovskite nanostructures (several atomic layers) have shown that the expected value of the effective piezomodulus is at the level of 0.1 C/m², which is in complete agreement with our results. Although our experiments are performed on macroscopic objects, we believe that the techniques being used highlight the surface contribution, specifically.

The appearance of a phase shift between $\tilde{E}_y$ and E_{ME} in such a scenario is also quite understandable on a qualitative level. The surface piezoelectric effect is formed at lengths that are comparable to the interatomic, and the phase of the associated response, up to electromagnetic delay, coincides with the phase u_{yy}. The region of bulk PE formation, including the magnetopiezoelectric, apparently extends over thicknesses δ, which are comparable to the wavelength, thus causing E_{ME} to lag relative to the surface response by a finite fraction of the period ($\psi_0 \sim q\delta$).

As noted above, the values physically recorded in the experiment are amplitudes and phases of the electric fields. Due to the linearity of the problem their relative changes coincide with the relative changes in the tensor components that are of interest to us, and therefore "tensor" terminology will be used from henceforth. The temperature variations of the complex parameter modulus $\kappa = e_{22}^{res}(T)/e_{y2}(T_N)$ are shown in Fig. 3. We divide κ into quadrature

$$\frac{e_{22}^{res}\sin\psi}{e_{y2}(T_N)} = \frac{e_{22}^{res}\sin\psi_0}{e_{y2}(T_N)} \qquad (5)$$

and in-phase

$$\frac{e_{22}^{res}\cos\psi}{e_{y2}(T_N)} = \frac{e_{y2}(T)}{e_{y2}(T_N)} + \frac{e_{22}^{eff}\cos\psi_0}{e_{y2}(T_N)} \qquad (6)$$

parts. The phase shift ψ_0 is close to $\pi/2$, and therefore the quadrature component is practically the same as $e_{22}^{eff}/e_{y2}(T_N)$ (Fig. 3). In order to find the temperature dependence $e_{y2}(T)$ it is necessary to know the most accurate value of ψ_0. We do not know how the surface PE is modified in the magnetically ordered state. If we assume that its variations are similar to the variations of the magnetopiezoelectric contribution
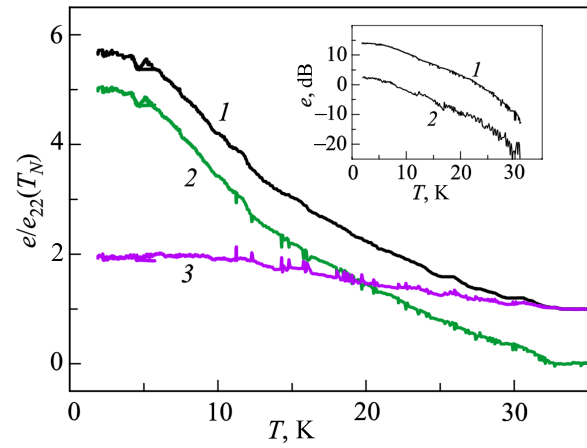

Fig. 3. The temperature changes of e_{22}^{res} (*1*), e_{22}^{eff} (*2*), and e_{y2} (*3*). All values are normalized to $e_{y2}(T_N)$. The inset shows the temperature dependences $e_{22}^{eff}/e_{y2}(T_N)$ (*1*) and $\delta e_{11}/e_{11}$ (*2*). The shift between curves is (13 ± 1) dB.

studied in Ref. 2, and that it increases approximately by a factor of two in the magnetically ordered phase, then we have to take ψ_0 in the interval ($75°$–$80°$).

Using Eqs. (2) and (3), for the dependences obtained at optimal φ_H we can write

$$\{\Delta e_{11}/e_{11}\}e_{11}/2e_{y2}(T_N) = \{e_{22}^{eff}/e_{y2}(T_N)\}.$$

The parameters measured directly in this equation are indicated by curly brackets and their temperature or magneto-field dependences must coincide with an accuracy up to a scale factor. Therefore, in logarithmic coordinates these dependences must be presented by congruent lines that are shifted by a value determined by the ratio between e_{11} and $e_{y2}(T_N)$. The inset in Fig. 3 demonstrates the validity of this conclusion. The shift is close to (13 ± 1) dB, which, taking into account 2 in the scale factor, gives the ratio $e_{11}/e_{y2}(T_N) \approx 10$. The direct measurements done by comparison give the same ratio, within error. The results presented in Fig. 2 are shown using this value with the stall parameter $\psi_0 = 80°$.

The magneto-field dependences of the amplitudes and phases of the signals measured at the optimum values of φ_H and $T = 1.7$ K are shown in Fig. 4. The results for the non-
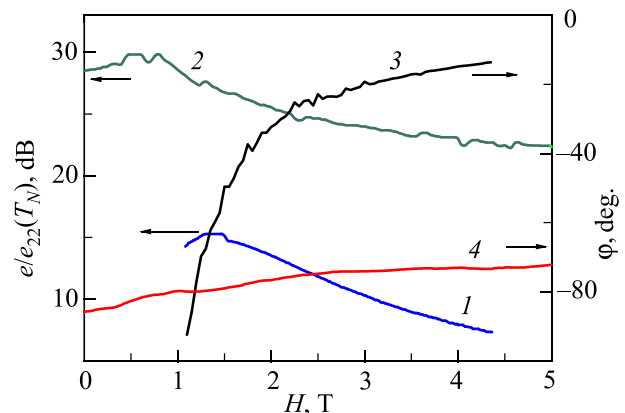

Fig. 4. The magneto-field dependences of the amplitudes (*1, 2*) and phases (*3, 4*) of the responses in a non-piezoactive (*1, 3*) and piezoactive (*2, 4*) configuration. $T = 1.7$ K. Normalization and the values of φ_H are the same as those in Fig. 2.
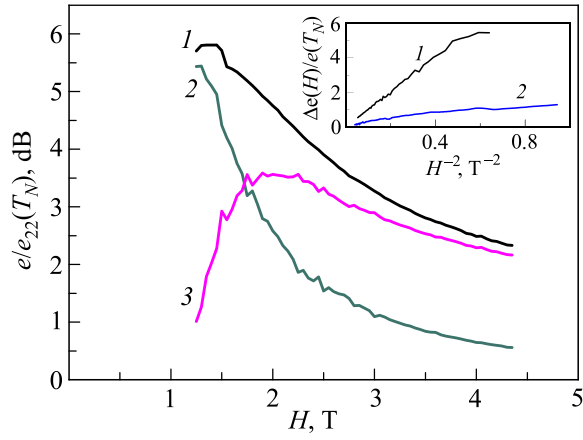
Fig. 5. The magneto-field variations e_{22}^{eff} (*1*), e_{22}^{eff} (*2*), and e_{y2} (*3*). All values are normalized to $e_{y2}(T_N)$. The inset is $e_{22}^{\text{eff}}/e_{22}(T_N)$ (*1*), $\Delta e_{11}/e_{11}$ (*2*). The ratio of slopes of the approximating lines (5 ± 0.5).

Fig. 6. Magneto-field changes to the speed of sound ($T = 1.7$ K) of the polarization u_{yy} (a) and u_{xx} (b). $\varphi_H = \pi/4$ (*1*), $\varphi_H = \pi/2$ (*2*), $\varphi_H = 0$ (*3*), the inset is the dependence $\Delta s/s$ (H^{-2}) upon excitation u_{yy} and $\varphi_H = \pi/4$.

piezoelectric configuration E_y, u_{yy} are presented only for the values H that exceed the spin-flop field. The mutual position of the curves on Fig. 4 for different configurations is determined in accordance with Fig. 2 at $T = 1.7$ K and $H = 1.4$ T. Just as before, we divide the resultant complex piezomodulus into in-phase and quadrature components (Fig. 5). The latter, according to Eqs. (2) and (3), should decrease with increasing H as the square of the magnetic field ($\partial^2\tilde{F}/\partial\varphi^2 \approx \chi H^2$), which is demonstrated by the inset in Fig. 5, well-approximated by the linear dependence H^{-2}. The same inset shows the analogous dependence for the increase of the piezoelectric modulus in the configuration E_x, u_{xx}. In the region of sufficiently large fields ($H > 2.5$ T) its change is also almost linear. The ratio of the slopes of these dependences (5 ± 0.5) agrees with the above estimate $e_{11}/e_{y2}(T_N)$.

Let us now discuss the behavior of the speed of the longitudinal sound in the configuration being discussed. In order to calculate it, similarly to Ref. 2, we find the derivative $d\sigma_{yy}/du_{yy}$, still taking into account the implicit dependence of φ on E and u. We also note that the speed of sound is a bulk characteristic, and the contribution of the surface effects is practically absent for the sample thicknesses used. As a result, for the change in the speed of sound we get the equation

$$\frac{\Delta s}{s} = -\frac{b^2 \sin^2 2\varphi}{\dfrac{\partial^2\tilde{F}}{\partial\varphi^2} + \dfrac{4\pi a^2}{\varepsilon_\perp}\cos^2 2\varphi}\frac{1}{2\rho s_{Ly}^2}. \qquad (7)$$

In Eq. (7) $\varepsilon_\perp$ is the dielectric permittivity of the paraphase in the reference plane, ρ is the density, s_{Ly} is the longitudinal sound velocity along the y axis.

The magneto-field dependences of the speed of sound in the configuration E_y, u_{yy} in comparison to the data for configuration E_x, u_{xx} are shown in Fig. 6. The spin-dependent contribution to the speed of sound in both configurations in a spin-flop state ($H > 1.5$ T) is maximal at $\varphi_H = \pi/4$. This agrees both with Eq. (7) and the corresponding expression for $\Delta s/s$, shown in Ref. 2. It can be seen that the scale of the effect in the first case is several times greater than for the second one. The reason for this is as follows. As demonstrated in Ref. 2, the behavior of $\Delta s/s$ is determined by two
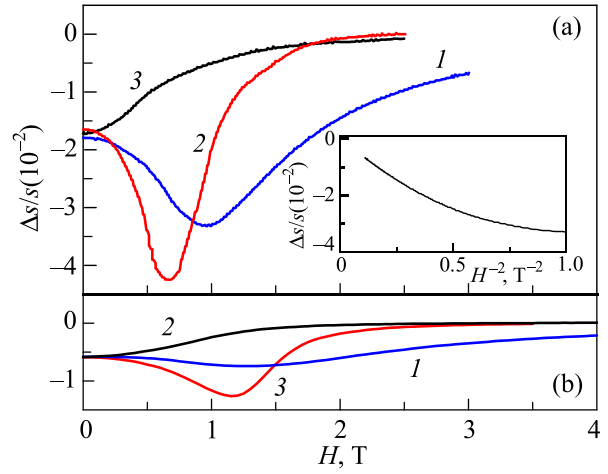
opposing factors, the tightening due to the renormalization of the piezoelectric modulus in the magnetically ordered phase and the softening due to magnetoelasticity. This conclusion is valid for any geometry in the experiment. On the x axis these two factors largely compensate for one another, at the same time as when on the y axis with $\varphi_H = \pi/4$ the contribution of the piezoelectric effect is completely suppressed and only the magnetoelastic interaction remains in its pure form. The high-field wing $\Delta s/s$ along the dependence H^{-2} is also straightened out in this case (see Fig. 6(a), inset). Using the value $\rho s_{Ly}^2 = 327$ GPa (Ref. 6) and $\chi = 5.4 \times 10^{-4}$ (Ref. 7) the slope of the linear approximation is used to obtain the value $b \approx 1.45 \times 10^7$ J/m^3. This value is close to the previous estimate in Ref. 2 ($b \approx 1.7 \times 10^7$ J/m^3).

From the results shown in Fig. 6 it can be seen that the speed of sound at $\mathbf{q}\|\mathbf{H}$ passes through a very deep minimum in the region of fields preceding the spin-flop transition. We believe that this effect is caused by the interaction of the sound and the domain walls that align orthogonally to the applied field in the pre-transitional region.

In conclusion, let us formulate the main results of the conducted research. The appearance of piezoelectricity in the non-piezoactive (in terms of paraphase) configuration of the multiferroic SmFe$_3$(BO$_3$)$_4$ is considered. Several piezoelectric effect channels are detected. Indirect PE appears in the single-domain phase of the antiferromagnets as a result of the combined action of the magnetoelectric and magnetoelastic mechanisms. We isolate the contribution to the studied dependences from the surface piezoelectric effect that exists in the paraphase and overtakes the bulk PE of any nature by a quarter of a period. Quantitatively, the value of the "surface" piezoelectric modulus is not small, and in terms of the order of magnitude it is consistent with the available theoretical estimates. We believe that this circumstance must be taken into account when working with nanoobjects. The change in the speed of longitudinal sound in the non-piezoactive configuration is measured, and turns out to be much larger than the analogous indicators in the opposite case, and it is shown that these features are well-described by the existing phenomenological expressions.

a)Email: fil@ilt.kharkov.ua

1L. D. Landau and E. M. Lifshitz, *Electrodynamics of Continuous Media* (Nauka, Moscow, 1982).

2T. N. Gaydamak, I. A. Gudim, G. A. Zvyagina, I. V. Bilych, N. G. Burma, K. R. Zhekov, and V. D. Fil, Phys. Rev. B **92**, 214428 (2015).

3I. V. Bilych, K. R. Zhekov, T. N. Gaidamak, I. A. Gudim, G. A. Zvyagina, and V. D. Fil, FNT **42**, 1419 (2016) [Low Temp. Phys. **42**, 1112 (2016)].

4P. Zubko, G. Catalan, and A. Tagantsev, Ann. Rev. Mater. Res. **43**, 387 (2013).

5S. Dai, M. Gharbi, P. Sharma, and H. S. Park, J. Appl. Phys. **110**, 104305 (2011).

6T. N. Gaidamak, I. A. Gudim, G. A. Zvyagina, I. V. Bilych, N. G. Burma, K. R. Zhekov, and V. D. Fil, FNT **41**, 792 (2015) [Low Temp. Phys. **41**, 614 (2015)].

7A. A. Mukhin, G. P. Vorobyev, V.Yu. Ivanov, A. M. Kadomtseva, A. S. Narizhnaya, A. M. Kuzmenko, U. F. Popov, L. N. Bezmaternykh, and I. A. Gudim, JETP Lett. **93**, 305 (2011).

Translated by A. Bronskaya